Journal of Biomechanical Science and Engineering

Vol.1, No.1, 2006

【Review Paper】

From Passive Motion of Capsules to Active Motion of Cells*

D. BARTHÈS-BIESEL**, T. YAMAGUCHI***, T. ISHIKAWA*** and E. LAC**

** Génie Biologique, Université de Technologie Compiègne
UMR CNRS 6600 Biomécanique et Génie Biomédical, BP 20529 - 60205 Compiègne cedex, France
E-mail: dbb@utc.fr

*** Dept. Bioeng. Robotics, Grad. Sch. Eng., Tohoku University
6-6-01, Aoba, Aramaki, Aoba-ku, Sendai 980-8579, Japan
E-mail: takami@pfsl.mech.tohoku.ac.jp

Abstract

In the past three decades, there has been great progress in the mathematical modeling and computational methods for fluid mechanics of suspensions of micron-scale particles. In medical or biological applications, the particles can be very deformable, self propelled or both. Research on mathematical and computational methods for the modelling of suspensions of such particles is currently very active. In this review paper, we introduce some of the concepts that are used to analyse suspensions of either passive deformable particles or active locomotive particles. To simplify matters, we consider simple model particles that are initially spherical. In one case, the particle is a liquid droplet enclosed by a thin deformable membrane (a 'capsule') and is deformed by hydrodynamic forces. In the other case, the particle remains spherical but propels itself by means of a velocity wave on its surface. Athough the basic equations for locomotive spherical cells and for capsules are similar, the resulting suspension characteristics are quite different owing to the different boundary conditions on the surface of the particles.

Key words : Capsule, Locomotive Cell, Stokes Flow, Hydrodynamic Interaction, Suspension

1. Introduction

In the past three decades, there has been great progress in the development of mathematical and computational models for the mechanics of suspensions of micron-scale particles. When the particles are rigid and non-Brownian, some efficient numerical approaches, such as Stokesian dynamics[(1)], the lattice Boltzmann method[(2)−(4)], the fast multipole method[(5)] allow to model efficiently the dynamics of a suspension of particles. In medical or biological applications however, the particles can be very deformable (e.g., red blood cells), self propelled (e.g., bacteria) or both. This adds considerable difficulties to the modelling of the dynamics of such particles and leads to active research on the development of mathematical and computational methods. In this review paper, we aim to introduce some of the concepts that are used to model suspensions of either passive deformable particles or active locomotive particles. To simplify matters, we consider simple model particles that are initially spherical. In one case, the particle is a liquid droplet enclosed by a thin deformable membrane (a 'capsule') and is deformed by hydrodynamic forces. In the other case, the particle remains spherical but propels itself by means of a velocity wave on its surface. Although the basic equations for locomotive spherical cells and for capsules are similar, the resulting suspension characteristics are quite different owing to the different boundary conditions on the surface of the particles.

These two cases correspond to two related fields of research where recent progress have been made. The study of encapsulated drops has applications in many industries like pharmaceutical, cosmetic, food industries for controlled release of active principles, aromas or

*Received 10 Aug., 2006 (No. R-06-B002)
[DOI: 10.1299/jbse.1.51]

flavours. They are also used for bioengineering applications like drug targeting or cell culture encapsulation for artificial organs[6]. Similarly, locomotion of cells in a suspension plays an important role in many physical and biological phenomena; such as plankton blooms in the oceans that affect the oceanic ecosystem, red tides in the coastal region that cause serious damage to fish farms, bioreactors for medicine or food, human digestion assisted by enterobacteria, ... In section 2, we present the mechanics of passive initially spherical capsules and show how the particle intrinsic physical properties affect its deformation in flow. We then present some first results obtained on the hydrodynamic interaction between two capsule in a semi-dilute suspension. In section 3, the basic equations for the locomotion of cells are explained, and the fluid mechanics of a dilute and concentrated suspension of locomotive cells is introduced.

2. Passive motion of spherical capsules in shear flow

A capsule consists of some internal medium enclosed by a semi-permeable membrane that controls exchanges between the environment and the internal contents and has thus a protection role. Natural capsules are cells, bacteria or eggs, but artificial capsules are widely used in many industries. Artificial capsules are usually obtained through interfacial polymerisation of a liquid droplet and are thus nearly spherical. The membranes that are used are natural or synthetic polymers such as poly-L-lysine, alginate or polyacrylates. In most situations, capsules are suspended into another liquid and are thus subjected to hydrodynamic forces when the suspension is flowing. The motion of the suspending and internal liquids creates viscous stresses on the membrane and may lead to capsule break-up. The control of this process is of course essential for the design of artificial capsules or for the protection of natural capsules but is difficult to achieve unless we have models of the underlying mechanics.

We focus here on artificial capsules that are initially spherical with an internal liquid core and that are enclosed by a very thin hyperelastic membrane. The mechanical properties of this membrane are essential in determining the motion and deformation of the capsule. We thus first present different constitutive laws that are commonly used to describe the rheological behaviour of thin membranes. We then consider the motion and deformation of a single capsule freely suspended in a simple shear flow and discuss the effect of the membrane constitutive law and of initial pre-stress. This situation is encountered in very dilute suspensions or in devices specially designed to measure the deformability of capsules[7],[8]. We then turn to the semi-dilute case and show how the hydrodynamic interactions between two identical capsules lead to large deformations and to irreversible trajectory shifts of the particles.

2.1. Membrane mechanics

The capsule is initially spherical with radius a. It is filled with a Newtonian incompressible liquid with viscosity $\mu^{(int)}$ and enclosed by an infinitely thin hyperelastic membrane with surface shear elastic modulus G_s and area dilation modulus K_s. We assume that the membrane is isotropic in its plane and thus that the principal directions of deformation and stress are colinear. The membrane constitutive law relates the principal elastic tensions (forces per unit arclength measured in the membrane plane) T_1 and T_2 to the two principal extension ratios λ_1 and λ_2. A number of laws have been proposed to model thin membranes, but we consider only the simplest ones with constant material coefficients. One candidate is the neo-Hookean law (NH) that corresponds to an infinitely thin sheet of a three-dimensional isotropic volume incompressible material

$$T_1 = \frac{G_s}{\lambda_1\lambda_2}\left[\lambda_1^2 - \frac{1}{(\lambda_1\lambda_2)^2}\right] \qquad (1)$$

Owing to the hypothesis of volume incompressibility, area dilation is balanced by membrane thinning and the area dilation modulus K_s is then shown to be $3G_s$[9]. Another approach consists in treating the membrane as a *two-dimensional* continuum with in-plane isotropy.

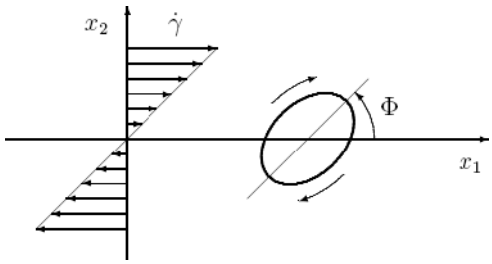

Fig. 1 Schematics of an isolated capsule freely suspended in a simple shear flow.

Correspondingly, starting from general principles of elasticity and thermodynamics, Skalak et al.[10] derived the following law (SK)

$$T_1 = \frac{G_s}{\lambda_1\lambda_2}\left[\lambda_1^2(\lambda_1^2-1) + C(\lambda_1\lambda_2)^2[(\lambda_1\lambda_2)^2-1]\right], \tag{2}$$

where the area dilation modulus is given by $K_s = G_s(1+2C)$. The SK law was initially designed to model the area incompressible membrane of biological cells such as red blood cells, corresponding to $C \gg 1$. However, this law is very general and can be used also to model other types of membranes for which K_s and G_s are of the same order of magnitude as is the case for alginate membranes[11]. The expression for T_2 is obtained by interchanging the roles of indices 1 and 2 in (1) and (2) . When $C = 1$, NH and SK laws predict the same small deformation behaviour of the membrane with $K_s = 3G_s$. However, they lead to different nonlinear tension-strain relations under large deformations. In particular, it is easily checked that NH law is strain softening under uniaxial stretching ($T_1 \neq 0$, $T_2 = 0$), whereas SK law is strain hardening[9].

2.2. Motion of a capsule freely suspended in linear shear flow

An initially spherical capsule is suspended in an unbounded shear flow with far field velocity $\mathbf{v}^\infty(\mathbf{x})$ and characteristic shear rate $\dot{\gamma}$ (figure 1). We use a reference frame centred on the capsule and moving with it. The unknown deformed surface of the capsule is denoted M. The internal (superscript $^{(int)}$) and external (superscript $^{(out)}$) liquids are Newtonian and have equal density ρ. The flow Reynolds number based on the capsule dimension is assumed to be very small $\rho\dot{\gamma}a^2/\mu^{(out)} \ll 1$, so that the motion of the internal and external liquids is governed by the Stokes equations

$$\begin{aligned} \nabla p^{(int)} &= \mu^{(int)}\nabla^2\mathbf{v}^{(int)} \quad , \quad \nabla.\mathbf{v}^{(int)} = 0; \\ \nabla p^{(out)} &= \mu^{(out)}\nabla^2\mathbf{v}^{(out)} \quad , \quad \nabla.\mathbf{v}^{(out)} = 0. \end{aligned} \tag{3}$$

Continuity between the internal and external velocities is imposed on M

$$\mathbf{v}^{(int)}(\mathbf{x},t) = \mathbf{v}^{(out)}(\mathbf{x},t) = \partial\mathbf{x}(\mathbf{X},t)/\partial t, \qquad \mathbf{x}\in M, \tag{4}$$

where $\mathbf{x}$ is the current position of a membrane material point that was at position $\mathbf{X}$ in the reference state. The membrane equilibrium equations relate the elastic tensions tensor $\mathbf{T}$ to the load due to the jump in viscous tractions across the interface

$$\nabla_s.\mathbf{T} + [\boldsymbol{\sigma}^{(out)}(\mathbf{x}) - \boldsymbol{\sigma}^{(int)}(\mathbf{x})].\mathbf{n} = 0, \qquad \mathbf{x}\in M, \tag{5}$$

where $\boldsymbol{\sigma}$ denotes the stress tensor in one of the liquids, $\mathbf{n}$ the outward unit normal vector to M and ∇_s the gradient along M. An important parameter of the problem is the ratio between viscous and elastic forces $\varepsilon = \mu^{out}\dot{\gamma}a/G_s$, that acts as an equivalent capillary number where surface tension is replaced by the membrane shear elastic modulus. For a given capsule, ε may also be viewed as a non-dimensional shear rate.

The solution of (3) to (5) with constitutive equation (1) or (2) is difficult to get, because the problem involves a strong coupling between fluid and solid mechanics, in the domain

where the shell deformations may be large and where the hydrodynamic forces are due to pressure and viscous shear stresses. When the capsule deformation is small, asymptotic solutions can be developed[12]. To first order in ε, the capsule takes an ellipsoidal shape, inclined at an angle $\Phi = 45^{\circ}$ with respect to the far field streamlines, while the membrane continuously rotates around the steady profile. In the case of large deformations, it is necessary to resort to numerical models. For thin membranes with negligible thickness, the boundary integral method is particularly well adapted and has been used extensively over the years[13]–[19]. The technique consists in first recasting the Stokes equations (3) in integral form. For the particular case where the viscosity of the two liquids are equal, $\mu^{(int)} = \mu^{(out)} = \mu$, as will be assumed hereafter, the interfacial velocity is given by[20]

$$\mathbf{v}(\mathbf{x}) = \mathbf{v}^{\infty}(\mathbf{x}) - \frac{1}{8\pi\mu} \oint_M \mathbf{J}(\mathbf{x},\mathbf{y}).[\boldsymbol{\sigma}^{(out)}(\mathbf{y}) - \boldsymbol{\sigma}^{(int)}(\mathbf{y})].\mathbf{n}(\mathbf{y})\, dS(\mathbf{y}), \tag{6}$$

where $\mathbf{v}^{\infty}(\mathbf{x})$ is the undisturbed simple shear flow and $\mathbf{J}$ the Oseen tensor for Stokes flow

$$J_{ij}(\mathbf{x},\mathbf{y}) = \frac{\delta_{ij}}{r} + \frac{r_i\, r_j}{r^3}, \tag{7}$$

with $\mathbf{r} = \mathbf{y} - \mathbf{x}$ and $r = \|\mathbf{r}\|$.

Then the usual technique of resolution consists in injecting the undeformed capsule in the flow field and in following numerically the time evolution of the capsule motion and deformation until a steady state is reached. At a given time, the position $\mathbf{x}(\mathbf{X}, t)$ of the membrane material points is thus known. By comparison with the initial reference state, the deformation and extension ratios of the capsule membrane are easily computed. Given a constitutive law (1) or (2), the equilibrium equation (5) leads to the value of the traction jump $[\boldsymbol{\sigma}^{(out)} - \boldsymbol{\sigma}^{(int)}].\mathbf{n}$ on the membrane. Then, for points $\mathbf{x}$ on M, the boundary integral equation (6) gives the velocity of the membrane points. The time integration of (4) leads to the new position of the membrane material points, and the process is repeated. From a purely numerical point of view, different discretisation techniques have been used, but the general principle is the same.

The validation of the numerical results is not easy. One way of doing it is to consider an intitially spherical capsule subjected to vanishingly small flow strength and to compare the numerical deformation to the asymptotic analytical deformation[12] developed for that case. Another check of numerical precision is done by monitoring the capsule volume during deformation and ensuring that it remains constant. Finally it is also useful to compare results obtained with different numerical procedures (see for example Lac et al.[22]).

2.3. Deformation of an initially unstressed capsule in a simple shear flow

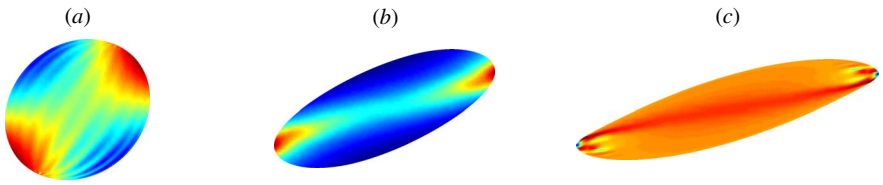

Fig. 2 Deformed profiles of a capsule in simple shear flow. (a) For low flow strength ($\varepsilon < \varepsilon_L$), the equilibrium profile is unstable and the membrane buckles. (b) For medium flow strength, the equilibrium profile is stable and the membrane rotates around the steady shape. (c) For high flow strength ($\varepsilon > \varepsilon_H$), no equilibrium profile is found and high curvature tips appear.

We now consider specifically the case of an initially *unstressed* capsule freely suspended in a simple shear flow with shear rate $\dot{\gamma}$ in the x_1, x_2 plane. The capsule deformation can be evaluated by means of the Taylor deformation parameter $D = (L - B)/(L + B)$ where L and B denote respectively the maximum and minimum profile diameters in the shear plane. This configuration has been studied for different shear rates and initial capsule shapes when the membrane obeys a neo-Hookean law[13],[16],[17],[21],[22]. Area incompressible membranes

Table 1 Minimum and maximum values of capillary number and deformation, for which steady equilibrium exists as functions of the membrane constitutive law (from Lac et al.[22]).

	NH	$SK(C = 0.5)$	$SK(C = 1)$	$SK(C = 10)$
ε_L	0.45	0.8	0.4	0.06
D_L	0.47	0.5	0.37	0.09
ε_H	0.63	≈ 1.2	2.4	≈ 7.5
D_H	0.53	≈ 0.55	0.6	0.61

have been considered to model the behaviour of red blood cells or lipid vesicles[16),(21),(23)] with non-spherical initial shapes. The bending rigidity of the membrane has also been taken into account[18),(23)].

Recently, Lac et al.[22] studied the effect of the membrane constitutive law on capsule deformation and compared NH and SK laws when the shear and area dilation modulus were of the same order of magnitude. They show that at shear rates lower than some critical value ε_L, the capsule reaches an equilibrium deformed state that is unstable owing to the presence of negative principal tensions. These cause membrane buckling because bending resistance has been neglected (figure 2a). Folds do occur and have been observed experimentally by Walter et al.[24] on spherical artificial capsules with a polysiloxane membrane ($G_s \approx K_s$). In that case, folds appear about the equator with the same orientation as those shown in figure 2a. As the shear rate increases, the membrane deformation and subsequent area dilation also increase and the tensions in the membrane become all positive. The capsule then reaches a steady deformed shape (figure 2b) with the membrane continuously rotating around it (*tank-treading* rotation), as has been reported experimentally[7),(8),(25)]. However, for large shear rates such that $\varepsilon > \varepsilon_H$, no equilibrium state seems to exist, the capsule exhibits high curvature tips and undergoes continuous extension until burst occurs (figure 2c). Such tips have also been observed experimentally for capsules with nylon membranes by Chang & Olbricht[7] right before break-up, albeit for small values of the viscosity ratio. The values of ε_L and ε_H, and of corresponding deformation D_L and D_H, depend on the membrane constitutive law as indicated in table 1. In particular, as we go from a strain-softening (NH) to an increasingly strain-hardening law (SK with increasing C), ε_L and D_L decrease, while ε_H increases significantly but D_H reaches an asymptotic value that is more or less independent of membrane law. It appears that the stability interval is quite narrow for NH and SK($C = 0.5$) laws. Accounting for a finite bending stiffness of the membrane, may remove the folds (depending on the bending modulus) and prevents the low shear instability. The steady deformed profile, however, then depends on the bending stiffness of the membrane. In particular, the tip curvature can be significantly decreased[19].

2.4. Deformation of a pre-stressed capsule in a simple shear flow

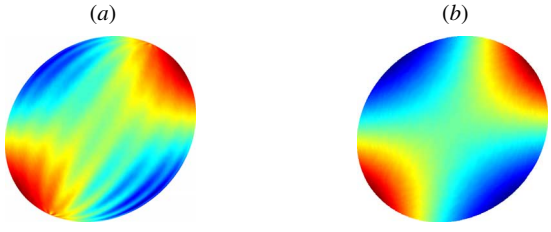

Fig. 3 A slight pre-inflation measured by α creates pre-stress in the membrane and may prevent buckling ($\varepsilon = 0.0375$); (a) $\alpha = 0$; (b) $\alpha = 1.5\%$

A positive pressure difference may occur between inside and outside of the capsule, particularly in bioengineering applications where the membrane is semipermeable, i.e., permeable to small molecules such as water or small ions but impermeable to large molecules[6]. The pressure difference is then due to osmotic effects. For example, in the case of a simple

capsule consisting of a drop of saline solution enclosed by an alginate membrane, some partial dissolution of the membrane occurs and leads to an unknown concentration of large molecules that are trapped inside the capsule[26]. As a consequence, the internal concentration is usually underestimated. Thus when the capsule is suspended in a saline solution with supposedly the same concentration as the internal medium, there exists a concentration jump across the membrane that leads to osmotic effects.

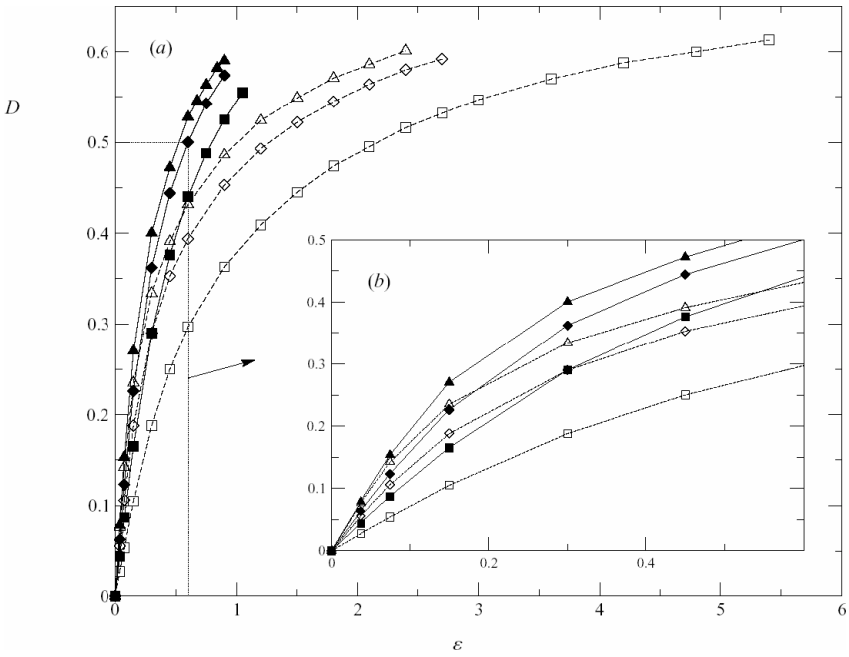

Fig. 4 Steady deformation in the shear plane as a function of pre-inflation and membrane constitutive law. △: $\alpha = 0$; ◊: $\alpha = 2.5\%$; □: $\alpha = 10\%$; filled symbols: NH law; open symbols: SK law ($C = 1$). Reproduced from Lac & Barthès-Biesel[27], Copyright 2005, American Institute of Physics

We thus now assume that the capsule is subjected to such a positive osmotic pressure difference $p^{(0)}$ between the internal and external phases. Consequently, since the capsule is spherical, the membrane is pre-stressed by an isotropic elastic tension $T^{(0)}$ given by the Laplace law

$$T_1 = T_2 = T^{(0)} = \frac{ap^{(0)}}{2}, \tag{8}$$

where a is the radius of the inflated capsule. The membrane is stretched with an initial isotropic elongation $\lambda_1 = \lambda_2 = a/a_0 = 1 + \alpha$, where a_0 is the capsule radius in the unstressed configuration. The relation between $T^{(0)}$ and α depends on the membrane constitutive law[27]. In particular, for a neo-Hookean membrane, $T^{(0)}$ is obtained from (1) and in the limit of small inflation, we find $T^{(0)} = 6\alpha G_s$. In all that follows, the capillary number ε will be based on the *inflated* capsule radius a, rather than the *unstressed* capsule radius a_0, because it is a that is usually measured. As shown by Lac & Barthès-Biesel[27], when such a pre-inflated capsule is suspended in a simple shear flow, the pre-stress can compensates the negative tensions that appear at low shear rates and membrane buckling can thus be avoided (figure 2.4). Altogether, the global effect of pre-stress is to decrease the capsule deformation for a given shear rate and to increase significantly the elastic tension in the membrane at a given deformation level. Furthermore, as shown in figure 4, the effects of pre-stress and of strain hardening add-up to decrease the membrane deformation for a given flow strength. Correspondingly, a capsule with a 10% pre-inflation and a SK membrane necessitate quite large values of capillary number ε to reach a 60% deformation. Lac & Barthès-Biesel[27] also show that for a preinflated

capsule, there is still a maximum shear rate ε_H above which no equilibrium could be found. The main effect of prestress is to increase slightly the value of ε_H.

2.5. Capsule interaction in simple shear flow

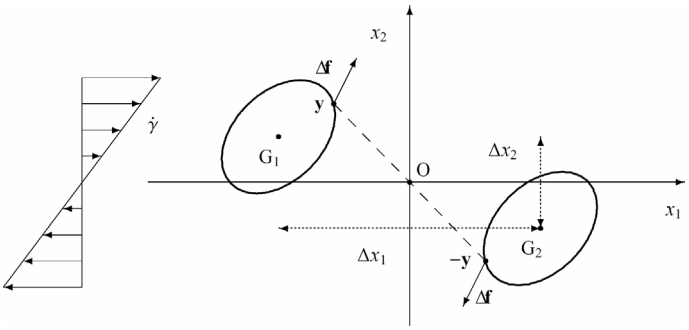

Fig. 5 Two capsules in simple shear flow

It is now of interest to consider the case of dilute suspensions of capsules and study the hydrodynamic interaction between capsules. The first study of this situation is due to Breyiannis & Pozrikidis[28], who modeled a two-dimensional suspension of capsules in simple shear flow for two surface fractions. They thus obtained a constitutive law for the two-dimensional suspension. However, the studies of a single capsule in shear flow all show that three-dimensional effects play an important role in determining the deformation and the tension distribution in the membrane.

Correspondingly, Lac et al.[29] considered the three-dimensional situation where two identical capsules interact in simple shear flow. The situation is the same as the one studied in sections 2.2 and 2.4, except that now there are two capsules (figure 5) with their centres of mass G_1 and G_2 located in the same shear plane x_1, x_2. The relative position of the two capsules is given by the vector $\Delta\mathbf{x}$:

$$\Delta\mathbf{x} = \mathbf{x}(G_1) - \mathbf{x}(G_2). \tag{9}$$

The capsule centres G_1 and G_2 are initially separated by $\Delta\mathbf{x}^0$. When $\Delta x_1^0 < 0$ and $\Delta x_2^0 > 0$ the capsules are naturally convected toward each other by the flow. The membrane obeys NH law and in order to avoid the buckling instability, the capsules are first slightly pre-stressed by inflation ($\alpha = 5\%$, $T^{(0)} \approx 0.254G_s$) with pre-inflated radius a. The problem solution follows essentially the same lines as for a single capsule, except that the integral in (6) has to be taken over the surfaces of the two capsules.

Lac et al.[29] find that the interaction remains weak as long as the distance between the two centres of mass is larger than a few initial capsule diameters. However, for small initial cross flow separations, the capsules deform a lot during the crossing over process. The corresponding sequences of capsule shapes are shown in figure 6 for two values of ε, corresponding to low ($\varepsilon = 0.75$) and high ($\varepsilon = 0.45$) flow strengths or equivalently to rigid or deformable particles. When $\Delta x_1/a \approx -3$, the capsules start to interact and their shapes are no longer exactly symmetrical with respect to their centre of mass (figure 6a, A). As separation decreases ($-3 \leqslant \Delta x_1/a \leqslant 0$), the centres of mass are shifted across streamlines and parts of the membranes flatten (figure 6b, c) or become concave (figure 6B, C). After crossing ($\Delta x_1 > 0$), the capsules are convected away from each other and the membranes recover a convex shape (figure 6d, D). For large separations $\Delta x_1/a > 7$, the hydrodynamic interaction between the particles is no longer visible and both capsules have relaxed to the steady deformed shape obtained for a single capsule subjected to the same flow conditions (figure 6e, E).

The hydrodynamic interaction leads to increased elastic tensions in the membrane in excess of 24% to 12% of the maximum tension in a single capsule. In most cases, the peak of tension in the membranes appears as the capsules overlap. However, for closely spaced

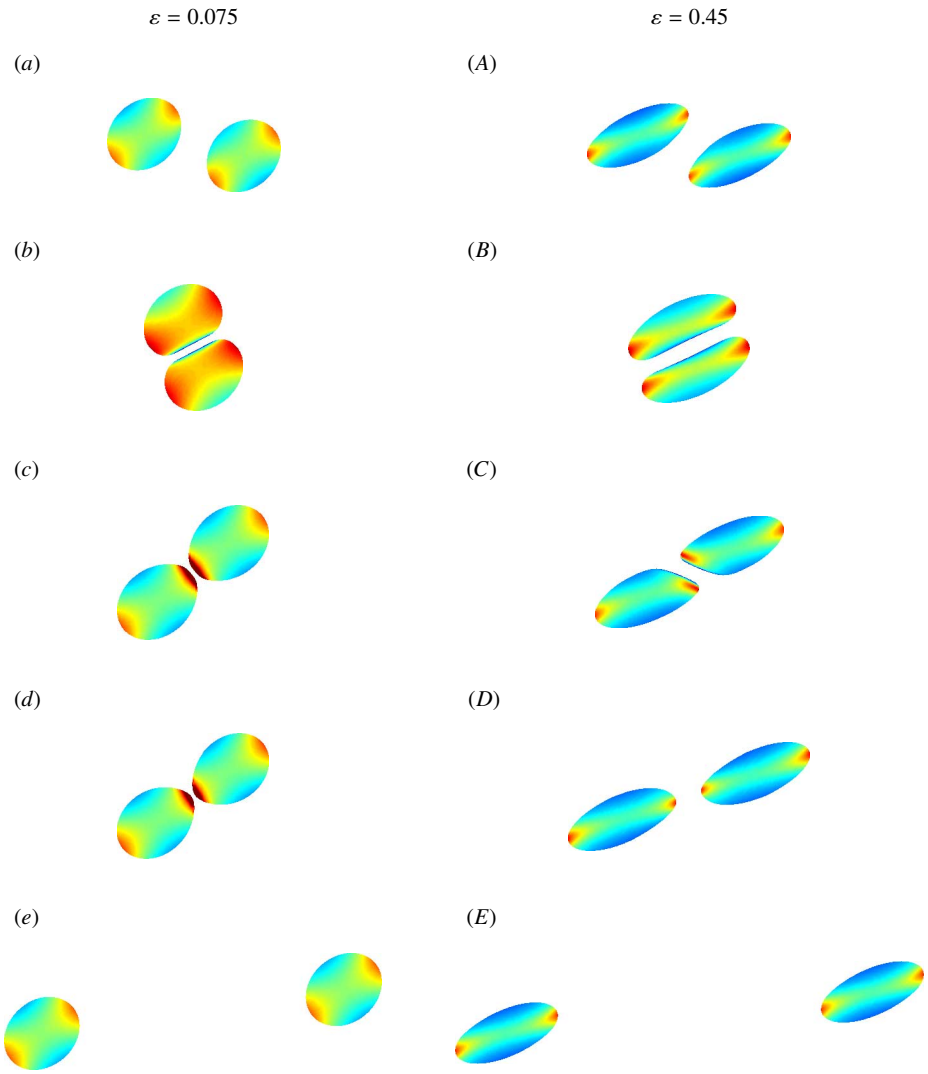

Fig. 6 Sequence showing, from top to bottom, the motion of two capsules for $\Delta x_2^0/a = 0.5$ and $\alpha = 5\%$; (*a–e*) $\varepsilon = 0.075$, $\Delta x_1^0/a = -8$; (*A–E*) $\varepsilon = 0.45$, $\Delta x_1^0/a = -10$. The color mapping corresponds to the normal load on the interface (scaling is different for the two sequences). From Lac et al.[29]

trajectories and small capillary numbers, high tensions appear in the near-contact regions during the separation phase. Such extra-tensions might damage the membranes. Even when the capsules are pre-inflated, the interaction generates negative tensions in the membrane (and thus possible buckling instabilities) in two different processes. For very small capillary number and preinflation ratio, the instability develops during the collision, as the capsules start overlapping. For high prestress levels ($\alpha \geqslant 2.5\%$ for a NH membrane), it appears above a maximum capillary number, as the two capsules separate and the membranes quickly evolve from a concave to a convex shape. This indicates that it would be quite interesting to include bending resistance in the membrane mechanical model to see how the post-buckling behaviour influences the particle interaction.

Furthermore, owing to the particle deformability and the inner and outer viscous flows, the collision is irreversible and the capsule separation increases after they have passed each other. The difference $\Delta x_2^{(f)} - \Delta x_2^{(0)}$ between the final and initial centre of mass separation can be as large as $0.6a$ when $\Delta x_2^{(0)} = 0.5a$. It decreases with capsule separation and is no very sensitive to flow strength. This irreversible trajectory shift must obviously lead to non-Newtonian and self diffusion effects in a semi-dilute suspension of identical capsules.

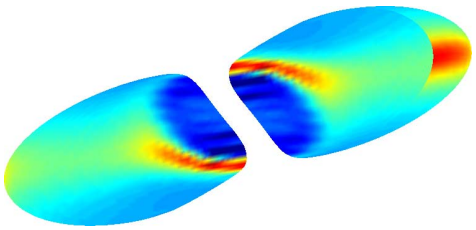

Fig. 7 Formation of folds in the flattened film during the separation phase. Each capsule has been artificially cut in half to show the film region. From Lac et al.[29]

There are a number of experimental studies of the collision of liquid droplets in different flow regimes. In particular for Stokes flow, high deformations as well as irreversible trajectory shifts are observed[30]. To our knowledge however, there is no published experimental study of the interaction of two capsules in shear flow. This is obviously a research domain that would be worth investigating.

2.6. Conclusion

Understanding and controlling the flow of a suspension of capsules represents an important challenge for many industrial processes. In particular, it is essential to ensure that no damage will occur when the particles are subjected to flow induced deformations. Presently, the few available theoretical results pertain essentially to an isolated capsule freely suspended in shear flow. They show that the membrane constitutive law plays an essential role in determining the capsule behaviour in shear flow. Another important parameter is the osmotic pressure inside the capsule that tends to rigidify the membrane while making it more fragile. It is clear that for membranes with a finite thickness, some bending rigidity must be taken into account. Bending resistance is the main membrane effect for lipid bi-layers that have very little shear elasticity. However, for thin hyperelastic membranes, the bending rigidity becomes important only when the ratio of thickness to curvature radius is larger than 0.1. This effect has not yet been studied in enough detail and it would be interesting to couple the roles of bending and of membrane constitutive law. The models developed for small or large deformations of a single capsule can be used to conduct an inverse analysis of experiments and thus obtain information on the mechanics of the capsule membrane[7],[8],[24],[25]. However, except for the pioneering work of Chang & Olbricht[7] there are very few experimental observations of flow induced burst, because the capsules were too resistant or the flow strengths not large enough. This is certainly a domain where more information is needed.

There are very few theoretical or experimental results regarding flow of a suspension of capsules, although this is a situation with many industrial or biological applications. The analysis of the hydrodynamic interaction between two capsules represents a first step in the direction of semi-dilute suspensions models. There is certainly need for powerful numerical techniques that can study the hydrodynamic interactions of a collection of capsules and predict the apparent viscosity of the suspension as well as the normal stress effects that are expected to occur. There is also need for experimental observations of interacting capsules.

3. Locomotion of cells

Another important characteristic of biological cells, other than the deformability, is the locomotion. Though the basic equations for the locomotive cells and those for capsules are similar, the output results of the suspension characteristics are quite different.

Modeling the locomotion of cells mathematically is a massive undertaking. Locomotive cells such as micro-organisms exist over a large range of length scales (roughly $1\,\mu m - 500\,\mu m$) and alter their behaviour depending on many parameters relating to their environment. The variety of shapes both inter- and intra-species is also vast. Any model capable of being analysed mathematically will therefore need to make severe simplifications.

A wide variety of fundamental models for locomotive cells have been proposed so far. The mathematical models for the locomotion of a solitary cell, such as a ciliate or a flagellant, were reviewed by Brennen[31], and the mathematical models for the mass transport around a locomotive cell were reviewed by Karp-Boss et al.[32]. To simplify matters, we focus on a *squirmer* model in the following sections (the details will be explicitly explained in section 3.1). We first present the basic equations and the motion of a solitary squirmer. We then consider the hydrodynamic interactions between two squirmers. This situation is encountered in the semi-dilute suspension. Finally, we present a integral property of a concentrated suspension of squirmers.

3.1. Locomotion of a solitary cell

Swimming speeds of locomotive cells such as micro-organisms range up to several hundred μm/s for the largest ones. However, the Reynolds number based on the swimming speed and the radius of individuals is usually less than 10^{-2}, so the flow field around the locomotive cells can be assumed to be Stokes flow with negligible inertia compared to viscous effects. Brownian motion is usually not taken into account, because typical locomotive cells are too large for Brownian effects to be important. Although our discussion is restricted to a solitary cell in this section, we present basic equations for many cells in order to utilise those in the following sections. When there are N cells in an infinite fluid, the Stokes flow field external to the cells can be given in integral form as[20),(33)]:

$$\boldsymbol{v}(\boldsymbol{x}) = \boldsymbol{v}^{\infty}(\boldsymbol{x}) - \sum_{i=1}^{N} \frac{1}{8\pi\mu} \int_{M_i} \boldsymbol{J}(\boldsymbol{x},\boldsymbol{y}).\boldsymbol{q}(\boldsymbol{y}) dS_i(\boldsymbol{y}) \tag{10}$$

where M_i is the surface of cell i, and $\boldsymbol{q}$ is the single-layer potential, which is same as the traction force on the surface if the cell shows rigid motion. This equation is analogous to equation (6) for a capsule, but in this case we considered N particles in the suspension.

The motions of locomotive cells are determined by the force conditions. When cell i is supposed to be subjected to known external forces $\boldsymbol{F}_i$ and torques $\boldsymbol{L}_i$, the equilibrium conditions for cell i are:

$$\boldsymbol{F}_i = \int_{M_i} \boldsymbol{q}(\boldsymbol{x}) dS_i, \ , \qquad \boldsymbol{L}_i = \int_{M_i} \boldsymbol{x} \wedge \boldsymbol{q}(\boldsymbol{x}) dS_i. \tag{11}$$

Locomotive cells are sometimes assumed to be neutrally buoyant, because the sedimentation velocity for typical aquatic micro-organisms is much less than the swimming speed, i.e. $\boldsymbol{F}_i = 0$. The centre of buoyancy of the cells may not coincide with its geometric centre, and in that case the torque $\boldsymbol{L}_i$ is generated. This tendency is called *bottom-heaviness*, and experi-

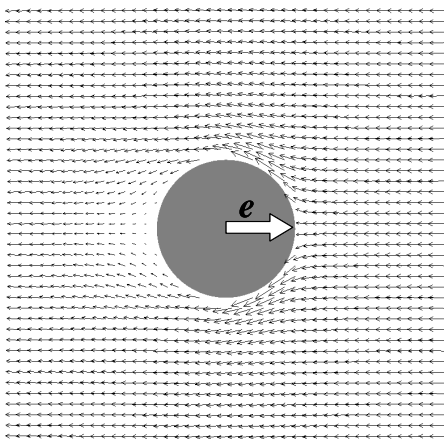

Fig. 8 Velocity vectors relative to the translational velocity vector of a squirmer. Uniform flow coming from far right. ($B_1 = B_2$)

mentally investigated by Kessler[34] for algae cells. Equations (10) and (11) can be solved by the boundary element method with specific boundary conditions on the cell surfaces[20),(33)].

The main difference between the capsules and the locomotive cells come from the boundary conditions. To simplify matters, we focus on a very simple cell model. Firstly we assume a spherical shape without any deformation. This assumption is made for obvious mathematical convenience, but a number of real micro-organisms, notably ciliates such as *Opalina* and colonies of flagellates such as *Volvox* are roughly spherical. Cyanobacteria also have no external appendages, and the cell body is approximately a spheroid with aspect ratio about two. Secondly, the cell model is assumed to propel itself by generating tangential velocities on its surface. In fact, it is a reasonable model to describe the locomotion of certain ciliates, which propel themselves by beating arrays of short hairs (cilia) on their surface in a synchronised way. In particular, the so-called symplectic metachronal wave employed by *Opalina*, for instance, in which the cilia tips remain close together at all times, can be modelled simply as the stretching and displacement of the surface formed by the envelope of these tips, and this can be regarded as approximately spherical[35),(36)]. The cell model swims due to the squirming motion on the surface, so it is referred to as a *squirmer*. The model of a squirmer was first proposed by Lighthill[37], and his analysis was then extended by Blake[35].

The tangential surface velocity on a squirmer up to the second mode may be given as;

$$\boldsymbol{v}_s = \sum_{n=1}^{2} \frac{2}{n(n+1)} B_n \left(\frac{\boldsymbol{e}.\boldsymbol{r}}{a} \frac{\boldsymbol{r}}{a} - \boldsymbol{e} \right) P_n'(\boldsymbol{e}.\boldsymbol{r}/a), \tag{12}$$

where P_n is the n^{th} Legendre polynomial, $\boldsymbol{e}$ is the unit orientation vector of a squirmer, $\boldsymbol{r}$ is the position vector and a is the radius. B_n is the strength of n^{th} swimming mode. The boundary condition for the squirmer is given by:

$$\boldsymbol{v}(\boldsymbol{x}) = \boldsymbol{V}_i + \boldsymbol{\Omega}_i \wedge (\boldsymbol{x} - \boldsymbol{x}_i) + \boldsymbol{v}_{s,i} \quad , \quad \boldsymbol{x} \in M, \tag{13}$$

where $\boldsymbol{V}_i$ and $\boldsymbol{\Omega}_i$ are the translational and rotational velocities of squirmer i. $\boldsymbol{x}_i$ is the centre of squirmer i, and $\boldsymbol{v}_{s,i}$ is the squirming velocity of squirmer i defined by (12). The swimming speed of a solitary squirmer is $2B_1/3$. The velocity field generated by a solitary squirmer with $B_1 = B_2$ is shown in figure 8 as an example.

3.2. Interactions between two squirmers

Two-cell interactions are the basics of many-cell interactions, thus it should be clarified before proceeding to the many-cell interactions. It is to be expected that in the presence of a nearby cell, a locomotive cell will not behave as if it were alone. It may consider reproducing sexually or attempting to consume (or avoid being consumed by) its neighbour. Ishikawa & Hota[38] experimentally investigated the interactions between two *Paramecium Caudatum*, in which the motion of cells were restricted between flat plates. The characteristics of a solitary *Paramecium* are well understood. Naitoh[39] investigated two kinds of biological reaction of a solitary *Paramecium* to mechanical stimulations. Avoiding reaction occurs when a cell bumps against a solid object with its anterior end. It does backward swimming first, then the cell gyrates about its posterior end, then resumes normal forward locomotion. Escape reaction occurs when the cell's posterior end is mechanically agitated. The cell increases its forward swimming velocity for a moment, then resumes normal forward locomotion. In the experiments by Ishikawa & Hota[38], they observed hydrodynamic interactions as well as avoiding and escape reactions. The results showed, however, that the cell-cell interactions were mainly hydrodynamic and the biological reactions were minor incidents.

There have been a few analytical investigations of hydrodynamic interactions between locomotive cells. Guell[40] discussed the flow field far from a spherical body with a rotating helical flagellum (modelling a swimming bacterium). Ramia[41] and Nasseri[42] also investigated the interaction between two spheroidal bodies with rotating helical flagella by using a boundary element method. Their computational conditions were limited to two cases, swimming side by side and swimming along one line. The minimum distance between the two

bodies was taken to be approximately equal to the minor axis of the spheroidal body, and they did not examine bodies in near contact. Lega and Passot[43] have derived a hydrodynamic model for bacterial colonies suspended on an agar plate. While including the modelling of nutrient transfer and hydrodynamics, the authors had to include an *ad hoc* interactive force acting between the micro-organisms. Thus, two micro-organisms in near contact were not analysed mechanistically in these former studies.

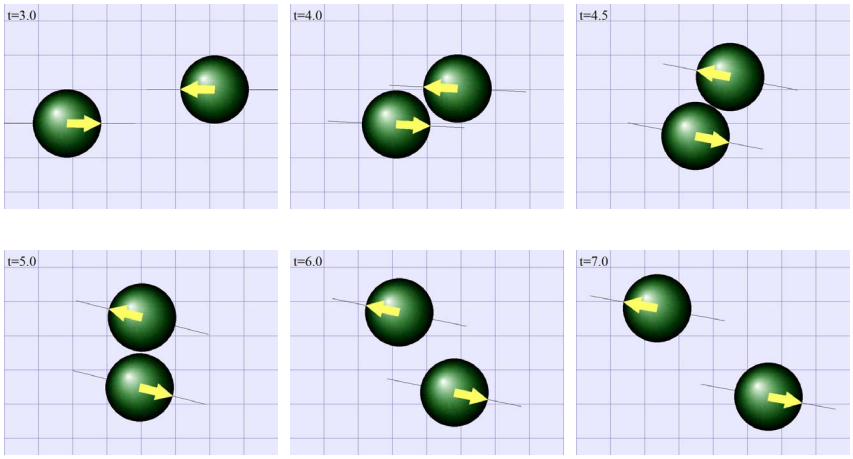

Fig. 9 Sequences showing the interactions between two squirmers initially facing each other ($B_1 = B_2$)

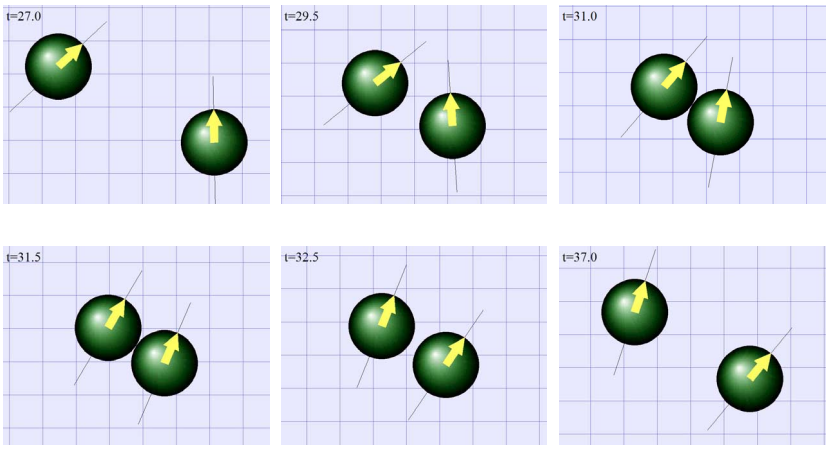

Fig. 10 Sequences showing the interactions between two squirmers whose orientation vectors initially have the angle of $\pi/4$ ($B_1 = B_2$)

The hydrodynamical interactions of pairs of squirmers, including two bodies in near contact, are reported by Ishikawa et al.[44]. Figure 9 shows the interactions between two squirmers initially facing each other, where t is the dimensionless time and $t = 0$ is the initial instant. The squirming motion of a sphere's surface is assumed to be invariant, so only the hydrodynamic interactions are considered. The orientation vectors of the squirmers are shown as big arrows on the spheres, and a thin solid line is added so that one can easily compare the angle between two squirmers. It is found from the figure that the two squirmers come very close to each other, then change their orientation in the near field, and finally move away from each other. The final directions of two squirmers are different from the initial directions in this case. Figure 10 also shows the interactions between two squirmers whose orientation vectors initially have the angle of $\pi/4$. Basically, the results of trajectories show that the squirmers attract each other at first, then they change their orientation dramatically when they are in near contact, and finally they separate from each other. The similar tendency is also observed in the experiment by Ishikawa & Hota[38] using *Paramecium*.

3.3. A concentrated suspension of squirmers

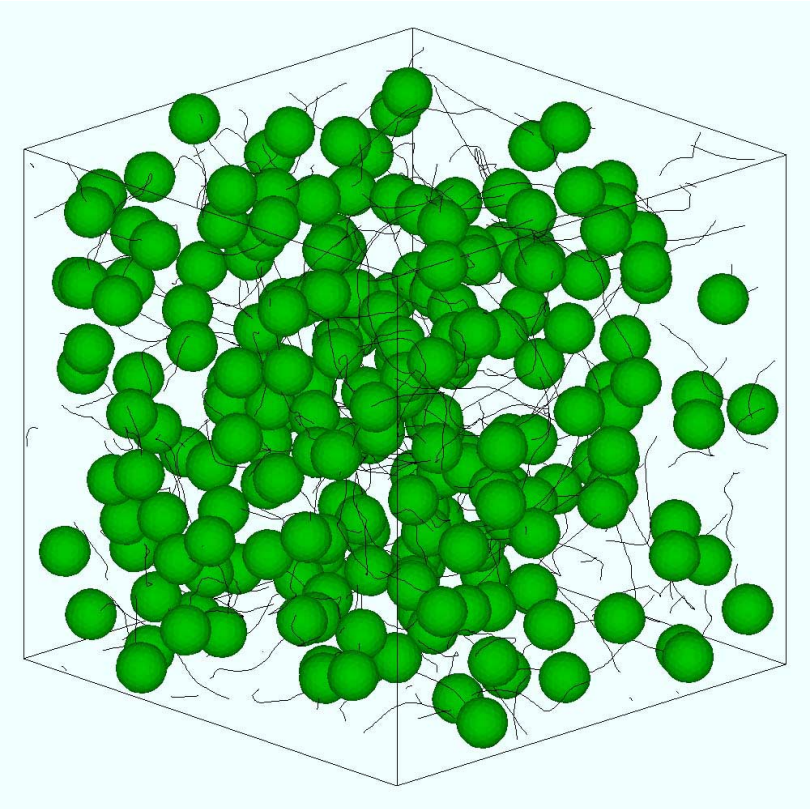

Fig. 11 Instantaneous positions of 216 identical squirmers with $B_1 = B_2$ in a fluid otherwise at rest. The volume fraction of cells is 10%. Solid lines are trajectories of the squirmers during the five previous time intervals.

Recently Dombrowski et al.[45] have reported a meso-scale structure in a concentrated suspension of *Bacillus subtilis*. In a concentrated suspension, a *B. subtilis* cell tends to swim in the same direction as its neighbours, generating a flow pattern larger than the scale of an individual cell but smaller than the scale of the container used in the experiment. The meso-scale structure changes its direction randomly in a manner reminiscent of turbulence, so they named this phenomenon *slow turbulence*. Mendelson et al.[46] also observed a meso-scale motion of whorls and jets generated by *B. subtilis*. The diffusivity of such a suspension was investigated experimentally by Wu and Libchaber[47]. They drew a stable two-dimensional soap film, and seeded bacteria (*Escherichia coli*) and micron-scale polystyrene beads in it. They investigated the effect of bacterial motion on the diffusivity of micron-scale beads in a freely suspended film, and the results showed that the diffusivity is 2-3 orders of magnitude larger than that of Brownian diffusivity. Since the meso-scale collective motions dramatically change the macro-scopic suspension property, it is important to clarify the microstructure in a suspension of locomotive cells.

The numerical simulation for the concentrated suspension of locomotive cells is currently one of the most challenging tasks in this research field. The main difficulty for this simulation is that the lubrication flows in the thin intercellular space have to be solved accurately as well as the large scale flow structure, so the scale of flow field to be solved diverges considerably. When the deformation of cells can be neglected, however, one can utilize the efficient numerical methods for rigid particles as explained in the introduction, even with the boundary conditions with the surface squirming velocities.

In the absence of Brownian motion and at negligible particle Reynolds number, the equation of motion for N particles suspended in a Newtonian solvent undergoing a bulk linear flow

field can be written in the general form as (see a standard text book by Kim and Karrila[48], for instance);

$$\begin{pmatrix} \boldsymbol{F} \\ \boldsymbol{L} \\ \boldsymbol{H} \end{pmatrix} = [\boldsymbol{R}] \begin{pmatrix} \boldsymbol{V} - \langle \boldsymbol{v} \rangle \\ \boldsymbol{\Omega} - \langle \boldsymbol{\omega} \rangle \\ -\langle \boldsymbol{E} \rangle \end{pmatrix} \tag{14}$$

where $\boldsymbol{F}, \boldsymbol{L}, \boldsymbol{H}$ are respectively the force, the torque, the stresslet, and $\langle \boldsymbol{E} \rangle$ is the rate of strain tensor of the bulk suspension. $\boldsymbol{R}$ is the grand resistant matrix, which is the invert of the grand mobility matrix. In the case of many body interactions, it is convenient to introduce the resistance (or mobility) matrix. Because the unknown parameters per particle, in this case, is just 11; whereas the standard boundary element method requires thousands of unknowns per particle, if one generates hundreds of boundary mesh per particle. The derivation of $\boldsymbol{R}$ for rigid and inert particles as well as accuracy of this method have been extensively discussed by Brady[1),49], the computational method so-called *Stokesian-dynamics*. The surface squirming motion can be included in this framework, but the detailed explanation is omitted here because it is far beyond the scope of this paper.

Ishikawa & Pedley[50] investigated the diffusive behaviour of swimming micro-organisms, in order to obtain a better continuum model for a cell suspension (for experimental studies, see[51)–53)]). The movement of 216 identical squirmers in a cubic region of fluid otherwise at rest, with periodic boundary conditions, are simulated by the Stokesian-dynamics with the help of a data-base of near-field pairwise interactions compiled by the boundary element method. The volume fraction of cells in this case is 10%. The instantaneous positions of the squirmers and their trajectories during five time intervals are shown in figure 11. It is found that the trajectories of squirmers are not straight, because the hydrodynamic interaction between squirmers generates translational-rotational velocities between them.

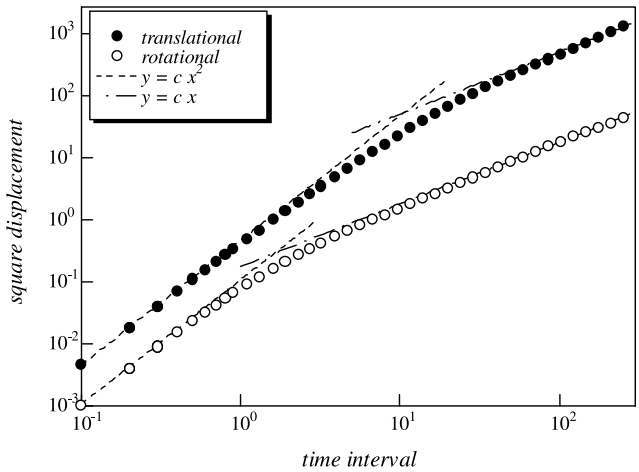

Fig. 12 Translational-rotational square displacement. When time interval is long enough, the square displacement and the time interval have the proportional connection.

In order to discuss the effective translational diffusivity, which is a measure of the increasing displacements between pairs of particles, one calculates the mean square displacement. If it grows more rapidly than linearly in time, then the spread is not diffusive (if proportional to t^2, it is as if the relative velocity of two spheres is constant), but if it becomes linear in time then the spread is diffusive. The results for the square displacement as a function of the elapsed time interval, are shown in figure 12. The square displacements linearly increase with square time interval for short time, which indicates that the translational and rotational velocities do not change so much during this short time interval. When the time interval is long enough, on the other hand, both translational and rotational square displacements linearly increase with time intervals. Therefore, the spreading of squirmers is correctly described as

a diffusive process over a sufficiently long time scale, even though all the movements of the individual squirmers are deterministically calculated.

3.4. Conclusion

The size of individual locomotive cell is often much smaller than that of the flow field of interest, so the suspension is usually modeled as a continuum in which the variables are volume-averaged quantities[54]–[58]. The continuum models proposed so far are, however, restricted to dilute suspensions. If one wishes to analyze a wide variety of suspensions, it will be necessary to consider the interactions between cells. Then the macro-scopic properties in the continuum model, such as the translational-rotational velocities of the locomotive cells, the particle stress tensor and the diffusion tensor, will need to be replaced by improved expressions. Though the introduced squirmer model is a very simple model, it can express macro-scopic properties of a suspension of locomotive cells, such as the effective diffusivity. We expect that such analysis will improve our understandings of the suspension and enable to predict a wide variety of phenomena in the suspension.

There are still a lot of difficulties in modeling and analyzing a suspension of real locomotive cells. One of them is the complex geometry of the cells. A bacterium, for instance, has several thin flagella composed of a helical protein, which has an amorphous core and a radius of about 10 – 20nm. These flagella change their shapes according to the locomotive motion, and sometimes associate in a flagellar bundle. Such complex shape change is the mechanism of the locomotion, however, it is not easy to analyze their motion mathematically and computationally. Another difficulty is the biological reaction of locomotive cells. As explained in section 3.2, even a solitary cell shows biological reactions to mechanical stimulations. The mechanism of such biological reactions has not been fully clarified, so the mathematical modeling of this phenomena is still an open question. Not only the mechanical stimulations but also chemical, optical, gravitational, electrical and magnetic stimulations may affect the locomotion of cells. These biological reactions also need to be taken into account in future work.

4. Concluding remarks

Two classes of biomechanical problems at the cellular scale have been presented. In one case, the particle is passive but highly deformable, while in the other case, the particle deformation is neglected but a mechanism for self propulsion is accounted for. When the cells are deformable and have an elastic surface such as a membrane, the unknown geometry of the particles has to be determined as part of the solution. This complicates the formulation of the problem and has prevented up to now the computation of the bulk properties of a suspension. The techniques presented here for *dilute* suspensions where only two capsules interact could be extended to suspension of red blood cells that are well represented by a capsule model with a non spherical initial geometry. The case of a more concentrated suspension is difficult to model and approximations must certainly be made if the computational cost is to be kept within reasonable limits.

For self propulsive particles, only simplified models with undeformable spherical cells allow for the computation of the behaviour of a collection of identical particles. The extension of the technique to non-spherical locomotive particles is feasible if difficult. A very challenging problem is the modelling of suspensions of *deformable* locomotive particles such as sperm and enterobacteria.

Consequently, better mathematical models and computational methods are needed for future developments in the study of suspensions of biological particles such as cells or bacteria. In particular, the case of heterogeneous suspensions containing particles with different sizes and properties represents a realistic situation that constitutes another modelling challenge.

Acknowledgements

The authors are grateful for helpful discussions about section 3 with Prof. T. J. Pedley in DAMTP, University of Cambridge.

This study was supported in part by the following grants: Grants-in-Aid for Scientific Research (A) by the Japan Society for the Promotion of Science (JSPS) No.16200031 (2004-2007) ; Grants-in-Aid for Scientific Research on Priority Areas, Biomechanics At Micro and Nanoscale Levels (Area No.768) No.15086204 (2003-2006) ; Tohoku University 21st Century Center of Excellence Programme "Future Medical Engineering Based on Bionanotechnology" (2002-2006) ; Special Coordination Funds for Promoting Science and Technology (Fostering talent in emergent research fields) No.42102 (2004-2008) ; The Institute of Industrial Science of the University of Tokyo, Revolutionary Simulation Software project (2005-2007) as the next-generation IT programs sponsored by the Ministry of Education, Culture, Sports, Science and Technology (MEXT).

References

(1) Brady, J. F. and Bossis, G., Stokesian dynamics, *Annu. Rev. Fluid Mech.* (1988), **20**, 111–157.

(2) Ladd, A.J.C., Numerical simulations of particlate suspensions via a discretized Boltzmann equation. Part 1. Theoretical foundation, *J. Fluid Mech* (1994a), **271**, pp.285-309.

(3) Ladd, A.J.C., Numerical simulations of particlate suspensions via a discretized Boltzmann equation. Part 2. Numerical results, *J. Fluid Mech* (1994b), **271**, pp.311-339.

(4) Ladd, A.J.C., Sedimentation of homogeneous suspensions of non-Brownian spheres, *Phys. Fluids* (1997) , **9**, pp.491-499.

(5) Sangani, A.S. and Mo, G., An O(N) algorithm for Stokes and Laplace interactions of particles, *Phys. Fluids* (1996) , **8**, pp. 1990-2010.

(6) Kuhtreiber W. M., Lanza R. P. and Chick W. L., *Cell encapsulation technology and therapeutics*, Birkhäuser (1998).

(7) Chang K. S and OlbrichtW. L. , Experimental studies of the deformation and breakup of a synthetic capsule in steady and unsteady simple shear flow, *J. Fluid Mech.* (1993), **250**, 609–633.

(8) Walter A., Rehage H. and Leonhard H., Shear-induced deformation of polyamid microcapsules, *Colloid Polymer Sci.* (2000), **278**, 169–175.

(9) Barthès-Biesel D., Diaz A. and Dhenin E., Effect of constitutive laws for two dimensional membranes on flow-induced capsule deformation *J. Fluid Mech.* (2002), **460**, 211–222.

(10) Skalak R., Tozeren A., Zarda R. P. and Chien S., Strain energy function of red blood cell membranes, *Biophys. J.* (1973), **13**, 245–264.

(11) Carin M., Barthès-Biesel D., Edwards-Levy F., Postel C. and Andrei C. D., Compression of biocompatible liquid filled HSA-alginte capsules: determination of the membrane mechanical properties *Biotech. Bioeng.* (2003), **82**, 207.

(12) Barthès-Biesel D. and Rallison J. M., The time-dependent deformation of a capsule freely suspended in a linear shear flow *J. Fluid Mech.* (1981), **113**, 251–267.

(13) Li X. Z., Barthès-Biesel D. and Helmy A., Large deformations and burst of a capsule freely suspended in an elongational flow *J. Fluid Mech.* (1988), **187**, 179–196.

(14) Pozrikidis C., Finite deformation of liquid capsules enclosed by elastic membranes in simple shear flow, *J. Fluid Mech.* (1995), **297**, 123–152.

(15) Zhou H. and Pozrikidis C., Deformation of capsules with incompressible interfaces in simple shear flow, *J. Fluid Mech.* (1995), **283**, 175–200.

(16) Ramanujan S. and Pozrikidis C., Deformation of liquid capsules enclosed by elastic membranes in simple shear flow: Large deformations and the effect of capsule viscosity, *J. Fluid Mech.* (1998), **361**, 117–143.

(17) Diaz A., Pelekasis N. A. and Barthès-Biesel D., Transient response of a capsule sub-

jected to varying flow conditions : effect of internal fluid viscosity and membrane elasticity *Phys. Fluids* (2000), **12**, 948–957.

(18) Kwak S. and Pozrikidis C., Effect of membrane bending stiffness on the deformation of capsules in uniaxial extensional flow, *Phys. Fluids* (2001), **13**, 1234–1242.

(19) Pozrikidis C., Effect of membrane bending stiffness on the deformation of capsules in simple shear flow, *J. Fluid Mech.* (2001), **440**, 269–291.

(20) Pozrikidis C., *Boundary integral and singularity methods for linearized viscous flow*, Cambridge University Press (1992).

(21) Eggleton C. D. and Popel A. S., Large deformation of red blood cell ghosts in a simple shear flow, *Phys. Fluids* (1998), **10**, 1834–1845.

(22) Lac E., Barthès-Biesel D., Pelekasis N. A. and Tsamopoulos J., Spherical capsules in three-dimensional unbounded Stokes flow: effect of the membrane constitutive law and onset of buckling *J. Fluid Mech.* (2004), **516**, 303–334.

(23) Kraus M., Wintz W., Seifert U. and Lipowsky R., Fluid vesicle in shear flow, *Phys. Rev. Lett.* (1996), **77**, 3685–3688.

(24) Walter A., Rehage H. and Leonhard H., Shear induced deformation of microcapsules: shape oscillations and membrane folding, *Colloids and Surfaces A: Physicochem. Eng. Aspects* (2001), **183–185**, 123–132.

(25) Rehage H., Husmann M. and Walter A., From two-dimensional model networks to microcapsules, *Rheol. Acta* (2002), **41**, 292.

(26) Sherwood J. D., Risso F., Collé-Paillot F., Edwards-Lévy F. and Lévy M. C., Transport rates through a capsule membrane to attain Donnan equilibrium *J. Colloid Interface Sci.* (2003), **263**, 202–212.

(27) Lac E. and Barthès-Biesel D., Deformation of a capsule in simple shear flow: effect of membrane prestress, *Phys. Fluids* (2005), **17**, 0721051–0721058.

(28) Breyiannis G. and Pozrikidis C., Simple shear flow of suspensions of elastic capsules. *Theor. and Comp. Fluid Dyn.* (2001), **13**, 327–347.

(29) Lac E., Morel A. and Barthès-Biesel D., Hydrodynamic interaction between two identical capsules in a simple shear flow, To appear in *J. Fluid Mech.* (2006),

(30) Guido S. and Simeone M., Binary collision of drops in shear flow by computer-assisted video optical microscopy. *J. Fluid Mech.* (1998), **357**, 1–20.

(31) Brennen, C. and Winet, H., Fluid mechanics of propulsion by cilia and flagella, *Annu. Rev. Fluid Mech.* (1977), **9**, 339–398.

(32) Karp-Boss L., Boss, E. and Jumars, P. A., Nutrient fluxes to planktonic osmotrophs in the presence of fluid motion, *Oceanography and Marine Biology: Annu. Rev.* (1996), **34**, 71–107.

(33) Youngren, G. K. and Acrivos, A., Stokes flow past a particle of arbitrary shape: a numerical method of solution, *J. Fluid Mech.* (1975), **69**, 377–403.

(34) Kessler, J. O., The external dynamics of swimming micro-organisms, *Progress in Phycological Research* (1986), ed. Round, F. E. and Chapman, D. J., **4**, 257–307. Bristol: Biopress

(35) Blake, J. R., A spherical envelope approach to ciliary propulsion, *J. Fluid Mech.* (1971), **46**, 199–208.

(36) Brennen, C., An oscillating-boundary-layer theory for ciliary propulsion *J. Fluid Mech.* (1974), **65**, 799–824.

(37) Lighthill, M. J., On the squirming motion of nearly spherical deformablr bodies through liquids at very small Reynolds numbers *Comm. Pure Appl. Math.* (1952), **5**, 109–118.

(38) Ishikawa, T. and Hota, M., Interaction of two swimming Paramecium, *J. Exp. Biol.* (2006), in press.

(39) Naitoh, Y. and Sugino, K., Ciliary movement and its control in *Paramecium*, *J. Protozool.* (1984), **31**, 31–40.

(40) Guell, D. C., Brenner, H., Frankel, R. B. and Hartman, H., Hydrodynamic forces and

band formation in swimming magnetotactic bacteria, *J. Theor. Biol.* (1988),**135**, 525–542.

(41) Ramia, M., Tullock, D. L. and Phan-Thien, N., The role of hydrodynamic interaction in the locomotion of microorganisms, *Biophysical J.* (1993), **65**, 755–778.

(42) Nasseri, S. and Phan-Thien, N., Hydrodynamic interaction between two nearby swimming micromachines, *Computational Mechanics* (1997), **20**, 551–559.

(43) Lega, J. and Passot, T., Hydrodynamics of bacterial colonies, *Phys. Rev.* E (2003), **67**, 1906.

(44) Ishikawa, T., Simmonds, M. P. and Pedley, T. J., Hydrodynamic interaction of two swimming model micro-organisms, *J. Fluid Mech.* (2006), in press.

(45) Dombrowski, C., Cisneros, L., Chatkaew, S., Goldstein, R. E. and Kessler, J. O., Self-Concentration and Large-Scale Coherence in Bacterial Dynamics, *Phys. Rev. Lett.* (2004), **93**, 098103.

(46) Mendelson, N. H., Bourque, A., Wilkening, K., Anderson, K. R. and Watkins, J. C., Organised cell swimming motions in Bacillus subtilis colonies: patterns of short-lived whirls and jets, *J. Bacteriol.* (1999), **180**, 600–609.

(47) Wu, Xiao-Lun & Libchaber, A., Particle diffusion in a quasi-two-dimensional bacterial bath, *Phys. Rev. Lett.* (2000), **84**, 3017–3020.

(48) Kim, S. & Karrila, S. J., *Microhydrodynamics: Principles and Selected Applications* (1992), Butterworth Heinemann.

(49) Durlofsky, L., Brady, J. F. and Bossis, G., Dynamic simulation of hydrodynamically interacting particles, *J. Fluid Mech.* (2004), **180**, 21–49.

(50) Ishikawa, T. and Pedley, T. J., An active suspension, *Mathematics Today* (2005), **41**, 84–86.

(51) Hill, N. A. and Häder, D. -P., A biased random walk model for the trajectories of swimming micro-organisms, *J. Theor. Biol.* (1997), **186**, 503–526.

(52) Vladimirov, V. A. *et al.*, Algal motility measured by a laser-based tracking method, *Mar. Freshwater Res.* (2000), **51**, 589–600.

(53) Vladimirov, V. A. *et al.*, Measurement of cell velocity distributions in populations of motile algae, *J. Exp. Biol.* (2004), **207**, 1203–1216.

(54) Bees, M. A. and Hill, N. A., Linear bioconvection in a suspension of randomly-swimming, gyrotactic micro-organisms, *Phys. Fluids* (1998), **10**, 1864–1881.

(55) Childress, S., Levandowsky, M. and Spiegel, E. A., Pattern formation in a suspension of swimming micro-organisms: equations and stability theory, *J. Fluid Mech.* (1975), **63**, 591–613.

(56) Hillesdon, A. J., Pedley, T. J. and Kessler, J. O., The development of concentration gradients in a suspension of chemotactic bacteria, *Bull. Math. Biol.* (1995), **57**, 299–344.

(57) Metcalfe, A. M. and Pedley, T. J., Falling plumes in bacterial bioconvection, *J. Fluid Mech.* (2001), **445**, 121–149.

(58) Pedley, T. J. and Kessler, J. O., A new continuum model for suspensions of gyrotactic micro-organisms, *J. Fluid Mech.* (1990), **212**, 155–182.